

Ratcheting boundary of pressurized pipe under reversed bending

Xiaohui Chen^{*1,2}, Xu Chen³ and Zifeng Li^{**2}

¹ School of Control Engineering, Northeastern University, Qinhuangdao, 066004, China

² School of Mechanical Engineering & Automation, Yanshan University, Qinhuangdao, 066004, China

³ School of Mechanical Engineering & Automation, School of Tianjin University, Tianjin, 300072, China

(Received November 7, 2018, Revised June 12, 2019, Accepted June 10, 2019)

Abstract. Ratcheting boundary is firstly determined by experiment, elastic-plastic finite element analysis combined with C-TDF and linear matching method, which is compared with ASME/KTA and RCC-MR. Moreover, based on elastic modulus adjustment procedure, a novel method is proposed to predict the ratcheting boundary for a pressurized pipe subjected to constant internal pressure and cyclic bending loading. Comparison of ratcheting boundary of elbow pipe determined by the proposed method, elastic-plastic finite element analysis combined with C-TDF and linear matching method, which indicates that the predicted results of the proposed method are in well agreement with those of linear matching method.

Keywords: pressurized pipe; finite element analysis; constitutive model; ratcheting boundary; elastic modulus adjustment procedure

1. Introduction

Ratcheting effect is defined as the accumulation of deformation or strain in structures/components under the action of cyclic loading. Last five years, ratcheting effect of pressurized pipe was studied by some researchers (Bradford and Tipping 2015, Nayebi and Hamidpour 2015, Nilsson *et al.* 2016, Kan *et al.* 2017, Varvani-Farahani and Nayebi 2017, Zakavi *et al.* 2017). Ratcheting behavior will reduce fatigue life of structures/components. The past several decades has seen a substantial increase in research into methods which calculate safe loading limits so that ratcheting does not occur, i.e., ratcheting boundary. In order to avoid ratcheting effect, it is necessary that ratcheting boundary is determined by the ratcheting criteria in standard code or the proposed simple method. The ratcheting effect has been considered in several standards, such as ASME (2017), KTA (2014) and RCC-MR (2007).

Ratcheting boundary was first investigated by Bree (1967, 1989) using a pressurized cylinder with cyclic thermal stresses across the wall thickness. The results gave Bree diagram, which had been contributed to the formation of the ratcheting criteria in ASME and KTA. RCC-MR code, which was an alternative to assume shakedown based on the test results. As the Practical Design Rule or Efficiency diagram rule was introduced into RCC-MR. Moreover, the Committee of Three Dimensional Finite Element Stress Evaluation (C-TDF) in Japan proposed one criterion for shakedown analysis with elastic-plastic finite element analysis, in which an elastic perfect plasticity

model or a bilinear kinematic hardening rule was used (Asada *et al.* 2002, Yamamoto *et al.* 2002).

Ratcheting boundary was studied by several scholars. On the hand, in terms of different experimental data in different positions, a regression technique was used to find a best fit straight line of the experimental data. The intercept of the fit straight line with the moment axis (i.e., zero ratcheting strain) was taken as the moment value required to initiate ratcheting strain. Moreton *et al.* (1996) proposed a method to determine ratcheting boundary of the pressurized elbow under cyclic bending loading. On the other hand, robust method (pseudo-elastic finite element analysis) is presented, such as linear matching method (LMM) (Ponter and Chen 2001, Chen *et al.* 2013), non-cyclic method (Reinhardt 2008, Peng *et al.* 2015), elastic modulus adjustment procedure (Adibi-Asl and Reinhardt 2010), hybrid method (Martin and Rice 2009), Uniform Modified Yield method (UMY) and “anisotropic” Load Dependent Yield Modification method (LDYM) (Abou-Hanna and McGreevy 2011), non-linear superposition method (Muscat *et al.* 2002), and some similar non-linear superposition methods (Abdalla *et al.* 2011, Adibi-Asl and Reinhardt 2010, Zheng *et al.* 2017, Konstantinos and Konstantinos 2012), namely simplified technique. Nayebi and Hamidpour (2015) studied shakedown and plastic, elastic shakedown and ratcheting limit of pipes with different types of defects under thermo-mechanical loading. Nonlinear kinematic hardening model of Armstrong-Frederick coupled with continuum damage mechanics was used and material properties were considered temperature-dependent. Interaction diagrams (Bree's diagram) of the defective pipelines were obtained and parametric studies involving different types and dimensions of part-through slot in the defective pipeline were investigated. Shen *et al.* (2018) proposed a new four-dimensional ratcheting boundary for the first time considering the interaction

*Corresponding author, Ph.D.,

E-mail: chenxh@neuq.edu.cn

**Co-corresponding author, Professor

among four types of stresses: constant mechanical membrane stress and mechanical bending stress, cyclic thermal membrane stress and thermal bending stress. On the basis of Tresca yield condition and elastic-perfectly plastic behavior, a novel two-plane FE model was built for numerical validation and results predicted by analytical solution agreed very well with that obtained by two-plane FE model. The relationship of the three-dimensional ratcheting boundary adopted by the newly implemented ASME VIII -2 Pressure Vessel Code and this four-dimensional ratcheting boundary considering constant mechanical membrane stress and mechanical bending stress, cyclic thermal membrane stress and thermal bending stress simultaneously was also discussed.

In the present paper, firstly, the ratcheting boundary for a pressurized pipe under reversed bending is determined with three methods, namely KTA/ASME code, efficiency diagram rule of RCC-MR and C-TDF method by elastic-plastic finite element analysis with the lightly AF type models. Secondly, based on the noncyclic method, a new ratcheting boundary determined method is established. Finally, the rationality and accuracy of the proposed method is verified.

2. Ratcheting boundary determination by codes

2.1 C-TDF

The C-TDF (Asada *et al.* 2002, Yamamoto *et al.* 2002) in Japan proposed one criteria to verify shakedown. The content of the criteria was that “Variations in equivalent plastic strain at the end of each cycle should have a decreasing trend and should become lower than the allowable limit of 10^{-4} /cycle”. Five or ten cycles were required to achieve this value. In this paper, ten cycles are used to determine ratcheting boundary of the pipes.

2.2 KTA/ASME code

For cylindrical vessels subjected to the load, but without secondary peak stresses, a formula for the ratcheting boundary is used which is adopted by KTA and based on

a curve given in ASME (Currently, the outer curve of figure T-1332-2 of ASME III-NH Appendix T):

While $X \leq 1.0$

$$Y = 3.25(1 - X) + 1.33(1 - X)^3 + 1.38(1 - X)^5 \quad (1)$$

where

$$X = \frac{P_m}{P_{sy}} \quad (2)$$

or

$$X = \frac{P_m + \frac{P_b}{K}}{P_{sy}} \quad (3)$$

where, P_{sy} corresponds to the pressure value at which the straight pipe with the same schedule yields at inner surface.

$$P_{sy} = \frac{K^2 - 1}{K^2 + 1} \sigma_y \quad (4)$$

where, $K = r_0/r_i$, r_0 and r_i is the outside radius and inside radius of pipe, respectively, σ_y is yield stress.

For a thin walled straight pipe or elbow under internal pressure, its primary membrane stress was expressed as the following.

$$P_m = \frac{KP}{K - 1} \quad (5)$$

where P is the applied internal pressure. So

$$X = \frac{KP}{(K - 1)P_{sy}} \quad (6)$$

Under bending loading range ΔF , the secondary bending stress range for the straight pipe is given by

$$\Delta Q = \frac{8\Delta F(l_o - l_i)D_o}{\pi(D_o^4 - D_i^4)} \quad (7)$$

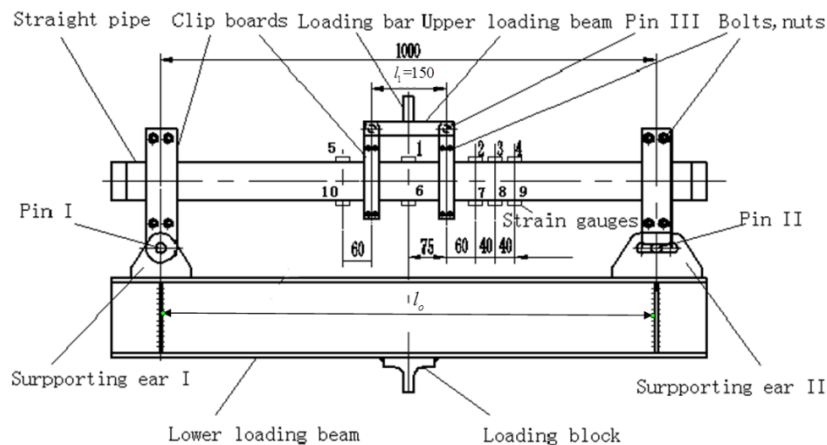


Fig. 1 Sketch of the quasi-three point bending apparatus and gauge positions (Chen *et al.* 2015)

where D_o and D_i are outer and inner diameter of the straight pipe, respectively; l_o and l_i are the spans of the lower and upper clips in Fig. 1, respectively. So

$$Y = \frac{\Delta Q}{P_{sy}} = \frac{8\Delta F(l_o - l_i)D_o}{\pi(D_o^4 - D_i^4)P_{sy}} \quad (8)$$

In the present paper, take straight pipe for example, the straight pipe made of Z2CND18.12N stainless steel were constructed of 76 mm diameter, 4.5 mm in nominal thickness, the length of straight pipe was 1000 mm (Chen *et al.* 2015), as given in Fig. 1. The pipe material properties are assumed to be temperature independent and isotropic. The elastic modulus $E = 195$ GPa, Poisson's ratio, $\nu = 0.3$, and yield strength, $\sigma_y = 360$ MPa.

Symmetry is used to model only one fourth of the straight pipe. The load case analysed is constant pressure P applied on inside surface of the straight pipe plus cyclic bending loading throughout the quasi-three-point bending positions.

The Finite Element Analysis model is shown in Fig. 2, in which only a quarter of the structure is included due to symmetry. Six hundred shell43 elements are used to mesh the pipe and 121 shell43 elements are used to mesh the end plate. In addition to the symmetric displacement constraints, displacement in the y -direction is applied to the central point of the end plate. Internal pressure is applied to the

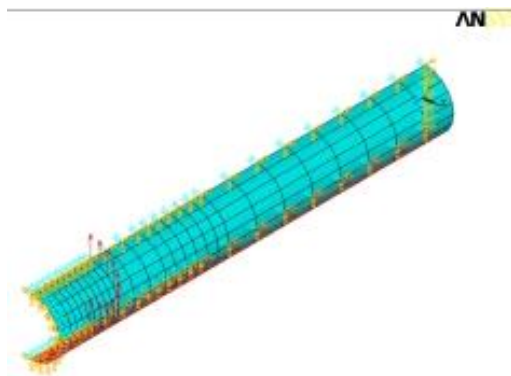


Fig. 2 Finite element analysis model of straight pipe

inside surface of the pipe and end plate. Reversed bending load or cyclic vertical displacement in the y -direction is distributed to nodes at the position corresponding to the central line of the clip board of the upper loading beam.

The ratcheting boundary of pressurized straight pipe shown in Fig. 3 in which all data were also transformed into X and Y by Eqs. (6)-(8). Fig. 3(a) gives the relationship of internal pressure and cyclic bending loading which are determined by bilinear kinematic hardening model (BKIN model) (Prager 1956), Chaboche model (CH3 model) (Chaboche 1986), Ohno-Wang II model (OW II model) (Ohno and Wang 1993) and Chen-Jiao-Kim model (CJK model) (Chen *et al.* 2005) combined with C-TDF. It is found that cyclic bending loading decreases with the increasing of internal pressure. Fig. 3(b) shows dimensionless form of ratcheting boundary of pressurized straight pipe subjected to reversed loading. Ratcheting boundary of pressurized straight pipe is compared with experimental data, C-TDF, ASME/KTA and RCC-MR. By comparing the experimental data, it indicates that ratcheting boundary determined by the C-TDF method with the lightly CJK model and RCC-MR describes the shakedown region well.

For a thin walled elbow under internal pressure

$$Y = \frac{\Delta F}{F_{sy}} \quad (9)$$

where, F_{sy} corresponds to the reversed bending loading at which the straight pipe with the same schedule yields at outside surface.

$$F_{sy} = \frac{\pi(r_o^4 - r_i^4)\sigma_y}{4r_o L_s \sin(\theta/2)} \quad (10)$$

where, L_s is the distance from the reversed bending loading point to the connecting section of straight pipe and elbow pipe, as given in Fig. 4, namely the moment arm of nominal reversed bending loading. θ is the angle of elbow pipe.

In the present paper, with 90° elbow pipe as an example, the 90° elbow specimens made of Z2CND18.12N stainless steel were constructed of 76 mm diameter, 4.5 mm in

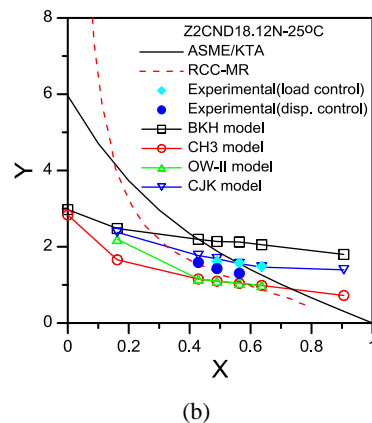
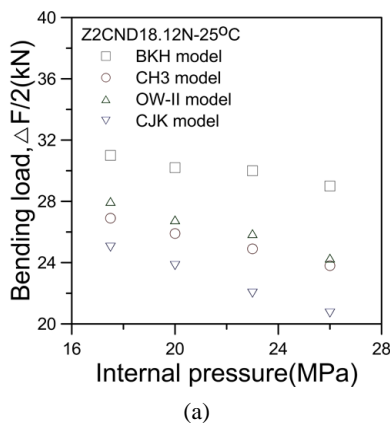


Fig. 3 Ratcheting boundary of pressurized straight pipe subjected to cyclic bending

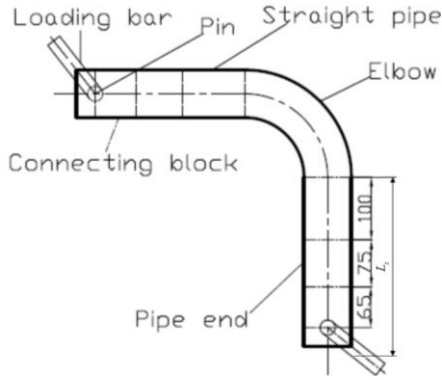


Fig. 4 Sketch of specimen (Chen *et al.* 2016)

nominal thickness, 90 degree, long radius (mean bend radius 95 mm) elbow pipe, each of which was butt welded to a 100 mm long straight pipe (Chen *et al.* 2016), as given in Fig. 4. The elbow material properties are assumed to be temperature independent and isotropic. The elastic modulus $E = 195$ GPa, Poisson's ratio, $\nu = 0.3$ and yield strength, $\sigma_y = 360$ MPa. The load case analysed is constant pressure P applied on inside surface of the pipe plus cyclic bending loading throughout the loading bar position.

Elbow pipes are classified by the bend angle and the bend radius. Elbow pipes that have a bend radius (R) that is 1.5 times or more the pipe mean diameter is termed long-radius elbow pipe. A schematic drawing of the finite element models is shown in Fig. 5. The model utilized in this study is a quarter model incorporating symmetry boundary conditions on two planes of symmetry; this model is used for pipe bends subjected to cyclic in-plane reversed bending. The pipe bend geometry is meshed with 4-noded plastic larger strain shell43 elements. The shell43 element has four integration points and six degrees of freedom at each node. The geometry of the quarter models is shown in Fig. 5(a). The quarter model (Fig. 5) has symmetry boundary conditions. The point of load application in the quarter model as shown in Fig. 5(b) is assigned a concentrated force.

Fig. 6 shows that the determined ratcheting boundary of elbow pipe by the C-TDF method based on OW II model with isotropic hardening rule is larger than that without isotropic hardening rule. Thus, the ratcheting boundary

determined by OW II model without isotropic hardening rule is on the conservative side.

2.3 Efficiency diagram rule of RCC-MR

According to the French RCC-MR, for the case of this study, only the ratio of secondary stress and membrane stress is concerned, and is determined by Eqs. (2) and (7).

$$SR_1 = \frac{\Delta Q}{P_m} \quad (11)$$

On the basis of experimental results, the correlation between the ratios of $\nu_1 = P_m/P_{eff1}$ and SR_1 are then determined

$$\nu_1 = \begin{cases} 1 & (SR_1 \leq 0.46) \\ 1.093 - \frac{0.926SR_1}{(1 + SR_1)^2} & (0.46 < SR_1 < 4) \\ \frac{1}{\sqrt{SR_1}} & (SR_1 \geq 4) \end{cases} \quad (12)$$

The effective primary stress can be calculated according to Eq. (13).

$$P_{eff1} = \frac{P_m}{\nu_1} \quad (13)$$

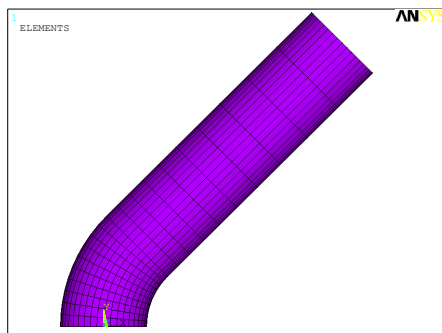
Limitation against shakedown is achieved with the aid of Eq. (14).

$$P_{eff1} \leq 1.2S_m \quad (14)$$

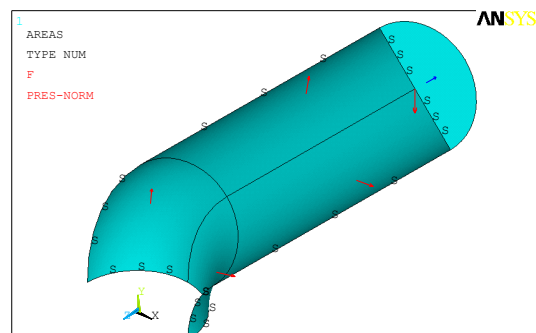
In order to compare with ratcheting boundary determined by ASME/KAT, the above method was changed as follows (Wolters *et al.* 1997).

For given primary stress according to Eq. (2) or Eq. (3), X is calculated, then

$$Y \leq \min \left(1.2\nu_1 SR_1 \frac{S_m}{S_y}; 1.2\nu_2 SR_2 \frac{S_m}{S_y} \right) \quad (15)$$

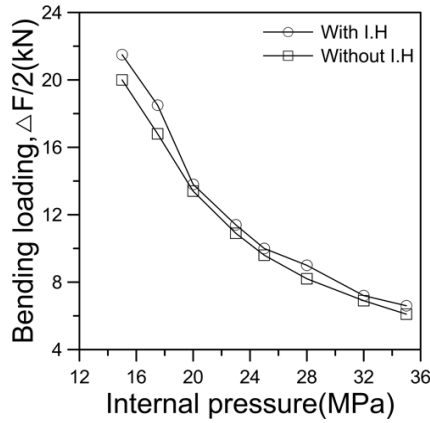


(a) Mesh

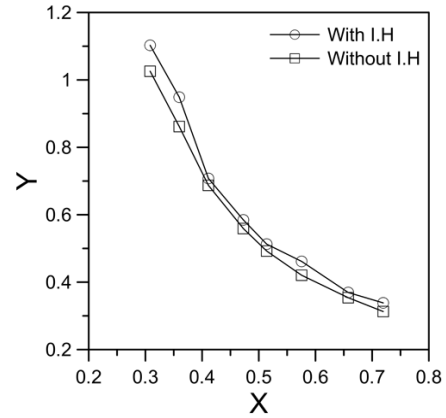


(b) Constrains and loads

Fig. 5 Finite element model



(a) Ratcheting boundary curve



(b) Dimensionless form of ratcheting boundary

Fig. 6 Ratcheting boundary

boundary of structural components is desirable. The

where

$$v_1 = \frac{P_m}{1.2S_m} \quad (16)$$

$$v_2 = \frac{X - \frac{P_m}{S_y} \left(1 - \frac{1}{K}\right)}{1.2 \frac{S_m}{S_y}} \quad (17)$$

And,

$$\text{When, } 1 \geq v > 0.5, \quad SR = \frac{\sqrt{1.093-v}}{v-0.167} \times (\sqrt{1.093-v} + \sqrt{0.926})$$

$$\text{When } 0.5 \geq v > 0, \quad SR = \frac{1}{v^2}$$

In fact, Eq. (15) are an implicit function of Y. The ratcheting boundary determined for the problem of this study is shown in Fig. 3.

2.4 Discussion

One criterion of C-TDF method is that 'Variations in equivalent plastic strain at the end of each cycle should have a decreasing trend and should become lower than the allowable limit of 10^{-4} /cycle.' The number of cycles required to achieve this value is not specified, but usually 5 or 10 cycles are needed. The ratcheting rate was based on the values of the first 10 cycles. C-TDF method determined ratcheting boundary, which need combine with elastic-plastic finite element analysis, i.e., ANSYS or ABAQUS step-by-step. However, it required considerable numerical expense and significant computer effort for complex structures. In order to avoid these shortcomings, a simple method should be developed.

At present, ratcheting boundaries are determined with the final aim of aiding the safety design and assessment of engineering piping structures, based on such experimental and FEA research. C-TDF method is commonly used to determine the ratcheting boundary of piping components. But it requires the scholar to repeat cycle-by-cycle in FEA. Therefore, an alternative method to predict the ratcheting

proposed non-cyclic methods are used to determine the ratcheting boundary of structural components. It is shown that these methods are simple, efficient and accurate for the given examples. In addition, these methods have made a great contribution for the progress of shakedown theory.

3. Proposed method

Ratcheting boundary of structures/components has been studied by many researchers. So far, few ratcheting boundary determination methods have been introduced into the codes and accepted by the scholars in various countries. Although not obvious so far, the limit analysis can be performed via a special case of shakedown analysis, where the cyclic load is reduced to monotonic load, the showdown and ratchet analysis can not be simply treated as a limit analysis. Therefore, on the basis of elastic modulus adjustment procedure in this study, a novel ratchet limit determination method is proposed based on their minds of Adibi-Asl and Reinhardt (2010), combined with Liu *et al.* (2009) and Reinhardt and Seshadri (2003). The contents of the proposed method are shown in the following.

- (1) Decompose the loading into steady (time-independent) primary P and zero-mean cycles $\Delta F/2$ components.
- (2) Create the finite element model by applying the load range of the cyclic load component (e.g. ΔF), with yield strength of ' $2\sigma_y$ '.
- (3) Obtain the von Mises stress distribution of each element $\Delta\sigma_{eq}$.
- (4) Create the finite element model by applying constant component P for limit load analysis.
- (5) Modify the elastic modulus at the element if von Mises stress of the element is larger than reference stress σ_{ref}^i .

$$E^{i+1} = \left(\frac{\sigma_{ref}^i}{\sigma_{eq}^i} \right)^{d_i} E^i \quad (18)$$

where, i is the iteration number ($i = 1$ for the initial elastic analysis), E^i is elastic modulus of i^{th} elastic iteration, E^{i+1} is elastic modulus of $(i+1)^{\text{th}}$ elastic iteration, σ_{eq}^i is von Mises stress of the element of i^{th} elastic iteration, σ_{ref}^i is reference stress of the element of i^{th} elastic iteration, q_i is the elastic modulus adjustment parameter.

The concept of reference stress was proposed by Seshadri and Mangalaramanan (1997). For inhomogenous material property, where yield strength is different all over the structures or components, the reference stress σ_{ref}^i is expressed in the following.

$$\sigma_{ref}^i = \left(\frac{\int_{V_T} \sigma_{eq}^2 dV}{\int_{V_T} \sigma_y^2 dV} \right)^{1/2} \sigma_y^i \quad (19)$$

For homogenous material property, where yield strength is different all over the structures or components, the reference stress σ_{ref}^i is expressed in the following.

$$\sigma_{ref}^i = \left(\frac{\int_{V_T} \sigma_{eq}^2 dV}{V_T} \right)^{1/2} \quad (20)$$

In order to obtain smooth convergence in the results, the elastic modulus adjustment parameter q_i can be varied systematically with von Mises stress and reference stress of the element. q_i is calculated from the respective linear elastic FEA solution in the following, as shown in Fig. 7.

$$q_i = \ln \left(\frac{2(\sigma_{ref}^i)^2}{(\sigma_{eq}^i)^2 + (\sigma_{ref}^i)^2} \right) / \ln \left(\frac{\sigma_{ref}^i}{\sigma_{eq}^i} \right) \quad (21)$$

- (6) Modify the yield strength at the above element by subtracting half of the von-Mises equivalent stress range from the original (cyclic) yield strength.

$$\sigma_y' = \sigma_y - \Delta\sigma_{eq} / 2 \quad (22)$$

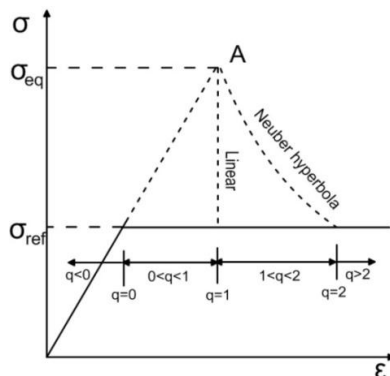


Fig. 7 Stress redistribution regions (Adibi-Asl *et al.* 2006)

- (7) Estimate the limit load multiplier m_α .

$$m_\alpha = 2m_2^0 \frac{2 \left(\frac{m_2^0}{m_L} \right)^2 + \sqrt{\frac{m_2^0}{m_L} \left(\frac{m_2^0}{m_L} - 1 \right)^2 \left(1 + \sqrt{2} - \frac{m_2^0}{m_L} \right) \left(\frac{m_2^0}{m_L} - 1 + \sqrt{2} \right)}}{\left(\left(\frac{m_2^0}{m_L} \right)^2 + 2 - \sqrt{5} \right) \left(\left(\frac{m_2^0}{m_L} \right)^2 + 2 + \sqrt{5} \right)} \quad (23)$$

$$m_2^0 = \sigma_y \frac{\sqrt{\int_{V_T} \left(\frac{\varepsilon_{eq}}{\sigma_{eq}} \right) dV}}{\sqrt{\int_{V_T} (\sigma_{eq} \varepsilon_{eq}) dV}} \quad (24)$$

where, σ_{eq} is von Mises stress of each element of each elastic iteration, ε_{eq} equivalent strain of each element of each elastic iteration.

$$m_L = \frac{\sigma_y}{(\sigma_{eq})_{\max}} \quad (25)$$

where, σ_y is modified yield strength of each element of each elastic iteration, $(\sigma_{eq})_{\max}$ is von Mises stress of each element of each elastic iteration.

Reinhardt and Seshadri (2003) discussed the limit load multiplier m_α . Two sides of Eq.20 divided by the exact multiplier m , provides

$$R_\alpha = 2R_0 \frac{2R_L^2 + \sqrt{R_L(R_L - 1)^2(1 + \sqrt{2} - R_L)(R_L - 1 + \sqrt{2})}}{(R_L^2 + 2 - \sqrt{5})(R_L^2 + 2 + \sqrt{5})} \quad (26)$$

where, $R_\alpha = m_\alpha/m$, $R_L = m_2^0/m_L$ and $R_0 = m_2^0/m$. m is the exact multiplier. m_L is lower bound limit load multiplier (Calladine 2000). m_2^0 is a new upper bound multiplier (Pan and Seshadri 2001). When $R_\alpha < 1$, m_α is lower limit load multiplier. When $R_\alpha > 1$, m_α is also upper limit load multiplier. When $R_\alpha = 1$, m_α is the boundary between lower limit load multiplier and upper limit load multiplier. Seshadri and Mangalaramanan (1997) thought that limit load multiplier m_α was closest to the exact multiplier m . Limit load multiplier m_α , also considers lower and upper limit theorem, which is a robust determined method of limit load multiplier.

The flowchart of the proposed method is shown in Fig. 8.

4. Cases analysis

With pressurized thick wall cylinder as an example, limit load of thick wall cylinder was determined by the proposed method, in order to the reliability of limit load determined by the proposed method. Internal diameter of thick wall cylinder R_i is 60 mm, outer diameter R_o is 180 mm. Elastic modulus is 200 GPa, yield strength σ_y is 300 MPa and internal pressure P is 50 MPa.

Theoretical value of limit load multiplier of pressurized

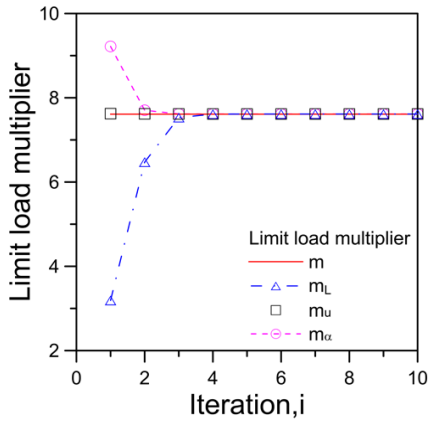
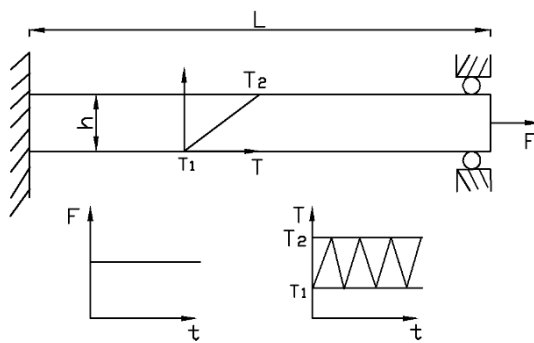


Fig. 10 Variation of limit load multiplier with iterations



(a) Schematic geometry and loading of Bree model



(b) Finite element mesh

Fig. 11 Classical Bree problem

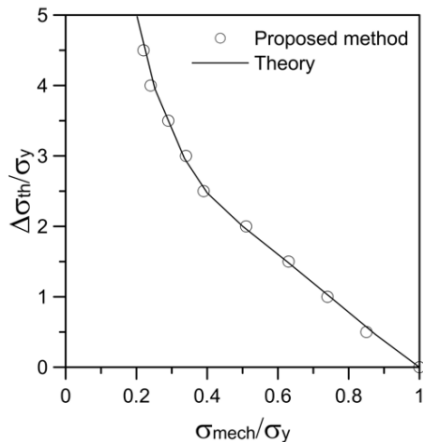


Fig. 12 Shakedown limit load of classical Bree problem

theoretical value of limit load multiplier. It is found that the proposed method is feasible. At the same time, calculated time required of the proposed method has a certain reduction.

In order to the reliability of ratchet limit determined by the proposed method, with Bree problem as an example (as

shown in Fig. 11), ratchet limit of Bree problem was determined by the proposed method, as given in Fig. 12. The results indicate that the proposed method is feasible.

5. Comparison

5.1 Ratcheting boundary of pressurized pipe

Fig. 13 shows ratcheting boundary of pressurized straight pipe which is determined by the experimental data, proposed method, C-TDF and ASME/KTA and RCC-MR code. It is shown in Fig. 13 that ratcheting boundary determined by the proposed method is in well agreement with that of C-TDF.

5.2 Ratcheting boundary of pressurized 90° elbow pipe

Ratcheting boundary of pressurized elbow pipe is given in Fig. 14. It indicates when $0.5 < X < 1$, ratcheting boundary determined by the proposed method is in well agreement with that of C-TDF; when $0.2 < X < 0.5$, ratcheting boundary determined by the proposed method is

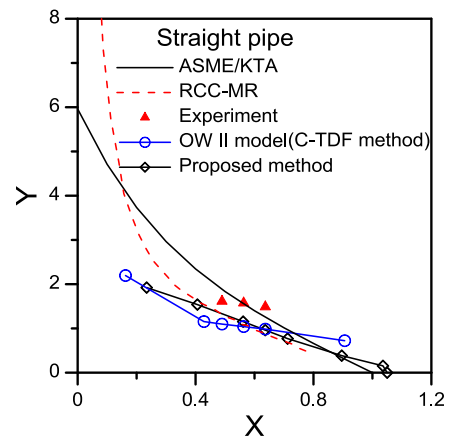


Fig. 13 Ratcheting boundary of straight pipe

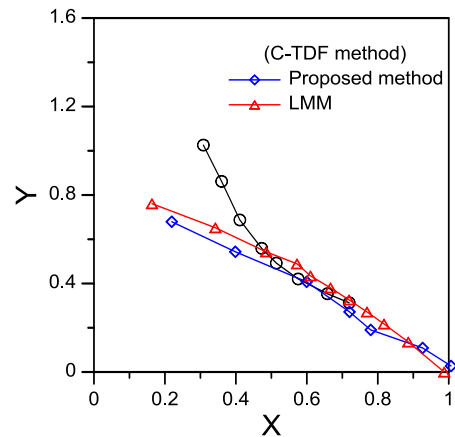


Fig. 14 Comparison of ratcheting boundary determined by the proposed method and LMM

inconsistent with that of C-TDF. This phenomenon was found by Abdalla *et al.* (2009) that used to simple technical method.

In order to verify the phenomenon, linear matching method is used to predict ratcheting boundary of 90° elbow pipe subjected to constant internal pressure and cyclic bending loading, as shown in Fig. 14. It is found that ratcheting boundary determined by the proposed method is in well agreement with that of LMM. Further, the reliability of the proposed method is verified.

6. Conclusions

Ratcheting boundary of 90° elbow pipe subjected to constant internal pressure and cyclic bending loading is firstly predicted by elastic-plastic finite element analysis combined with C-TDF method. The C-TDF method need repeated trial calculation, time-consuming. In order to quickly determine ratcheting limit, a novel method is proposed based on elastic modulus adjustment procedure in this study. And than the proposed method is used to determine ratcheting boundary of 90° elbow pipe. The results indicate that the proposed method is fast and efficient. Comparison of ratcheting boundary of 90° elbow pipe determined by proposed method with that of C-TDF method, which indicated when $0.5 < X < 1$, ratcheting boundary determined by the proposed method is in well agreement with that of C-TDF; when $0.2 < X < 0.5$, ratcheting boundary determined by the proposed method is inconsistent with that of C-TDF. In order to verify the phenomenon, LMM is used to predict ratcheting boundary of 90° elbow pipe subjected to constant internal pressure and cyclic bending loading. It is found that ratcheting boundary determined by the proposed method is in well agreement with that of LMM. Further, the reliability of the proposed method is verified.

Acknowledgments

This work was partly supported by the Natural Science Foundation of Hebei Province of China (No. E2018501022), China Postdoctoral Science Foundation Funded Project (No. 2017M610171) and Fundamental Research Funds for the Central Universities (No. N182304009).

References

- Abdalla, H.F., Megahed, M.M. and Younan, M.Y. (2009), "Comparison of pipe bend ratcheting/ shakedown test results with the shakedown boundary determined via a simplified technique", *Proceedings of the ASME – PVP Division Conference*, Prague, Czech Republic.
- Abdalla, H.F., Megahed, M.M. and Younan, M.Y.A. (2011), "A simplified technique for shakedown limit load determination of a large square plate with a small central hole under cyclic biaxial loading", *Nuclear Eng. Des.*, **241**, 657-665. <https://doi.org/10.1016/j.nucengdes.2010.11.019>
- Abou-Hanna, J. and McGreevy, T.E. (2011), "A simplified ratcheting limit method based on limit analysis using modified yield surface", *Int. J. Pres. Ves. Pip.*, **88**, 11-18. <https://doi.org/10.1016/j.ijpvp.2010.12.001>
- Adibi-Asl, R. and Reinhardt, W. (2010), "Ratchet boundary determination using a noncyclic method", *J. Press. Vess. – T. ASME*, **132**, 021201. <https://doi.org/10.1115/1.4000506>
- Adibi-Asl, R., Fanous, I.F.Z. and Seshadri, R. (2006), "Elastic modulus adjustment procedures improved convergence schemes", *Int. J. Pres. Ves. Pip.*, **83**, 154-160. <https://doi.org/10.1016/j.ijpvp.2005.11.002>
- Asada, S., Yamashita, N., Okamoto, A. and Nishiguchi, I. (2002), "Verification of alternative criteria for shakedown evaluation using flat head vessel", *ASME PVP*, **439**, 17-22. <https://doi.org/10.1115/PVP2002-1217>
- ASME (2017), ASME boiler and pressure vessel code, section III; American Society of Mechanical Engineer, New York, USA.
- Bradford, R.A.W. and Tipping, D.J. (2015), "The ratchet-shakedown diagram for a thin pressurised pipe subject to additional axial load and cyclic secondary global bending", *Int. J. Pres. Ves. Pip.*, **134**, 92-100. <https://doi.org/10.1016/j.ijpvp.2015.08.008>
- Bree, J. (1967), "Elastic-plastic behaviour of thin tubes subjected to internal pressure and intermittent high-heat fluxes with application to fast-nuclear-reactor fuel elements", *J. Strain Anal. Eng.*, **2**, 226-238. <https://doi.org/10.1243/03093247V023226>
- Bree, J. (1989), "Plastic deformation of a closed tube due to interaction of pressure stresses and cyclic thermal stresses", *Int. J. Mech. Sci.*, **31**, 865-892. [https://doi.org/10.1016/0020-7403\(89\)90030-1](https://doi.org/10.1016/0020-7403(89)90030-1)
- Calladine, C.R. (2000), *Plasticity for Engineers*, Horwood Publishing, Chichester, UK.
- Chaboche, J.L. (1986), "Time-independent constitutive theories for cyclic plasticity", *Int. J. Plast.*, **2**, 149-188. [https://doi.org/10.1016/0749-6419\(86\)90010-0](https://doi.org/10.1016/0749-6419(86)90010-0)
- Chen, X., Jiao, R. and Kim, K.S. (2005), "On the Ohno-Wang kinematic hardening rules for multiaxial ratcheting modeling of medium carbon steel", *Int. J. Plast.*, **21**, 161-184. <https://doi.org/10.1016/j.ijplas.2004.05.005>
- Chen, H.F., Ure, J.M. and Tipping, D. (2013), "Calculation of a lower bound ratchet limit part 1 – Theory, numerical implementation and verification", *Eur. J. of Mechanics / A Solids*, **37**, 361-368. <https://doi.org/10.1016/j.euromechsol.2012.04.001>
- Chen, X.H., Chen, X., Chen, G. and Li, D.M. (2015), "Ratcheting behavior of pressurized Z2CND18.12N stainless steel pipe under different control modes", *Steel Compos. Struct., Int. J.*, **18**(1), 29-50. <https://doi.org/10.12989/scs.2015.18.1.029>
- Chen, X.H., Chen, X., Chen, G. and Li, D.M. (2016), "Evaluation of AF type cyclic plasticity models in ratcheting simulation of pressurized elbow pipes under reversed bending", *Steel Compos. Struct., Int. J.*, **21**(4), 703-753. <http://dx.doi.org/10.12989/scs.2016.21.4.703>
- Kan, Q.H., Li, J., Jiang, H. and Kang, G.Z. (2017), "An Improved Thermo-Ratcheting Boundary of Pressure Pipeline", *Key Eng. Mater.*, **725**, 311-315. <https://doi.org/10.4028/www.scientific.net/KEM.725.311>
- Konstantinos, V.S. and Konstantinos, D.P. (2012), "A direct method to predict cyclic steady states of elastoplastic structures", *Compos. Method Appl. Mech. Eng.*, **223-224**, 186-198. <https://doi.org/10.1016/j.cma.2012.03.004>
- KTA (2014), "Kerntechnischer Ausschluß; Sicherheitstechnische Regel des KTA, Komponenten des primärkreises von Leichtwasserreaktoren", Teil: Auslegung, Konstruktion und Berechnung, Regeländerungsentwurf.
- Liu, Y.H., Chen, L.J. and Xu, B.Y. (2009), "Modified elastic compensation method for limit analysis of complex structures",

- Pres. Ves. Technology*, **26**(10), 10-16. [In Chinese]
- Martin, M. and Rice, D. (2009), "A Hybrid Procedure for Ratchet Boundary Prediction", *ASME PVP Conference*, Prague, Czech Republic.
- Moreton, D.G., Yahiaoui, K. and Moffat, D.G. (1996), "Onset of ratcheting in pressurized piping elbows subjected to in-plane bending moments", *Int. J. Pres. Ves. Pip.*, **68**, 73-79. [https://doi.org/10.1016/0308-0161\(94\)00041-7](https://doi.org/10.1016/0308-0161(94)00041-7)
- Muscat, M., Hamilton, R. and Boyle, J.T. (2002), "Shakedown analysis for complex loading using superposition", *J. Strain Analysis*, **37** (5), 399-412. <https://doi.org/10.1243/030932402760203865>
- Nayebi, A. and Hamidpour, M. (2015), "Thermo-mechanical cyclic loading analysis of pipes with different type of defects: Temperature dependent properties", *P.I. Mech. Eng. L – J. Mater.*, **230**, 303-310. <https://doi.org/10.1177/1464420715571432>
- Nilsson, K.F., Dolci, F., Seldis, T., Ripplinger, S., Grah, A. and Simonovski, I. (2016), "Assessment of thermal fatigue life for 316L and P91 pipe components at elevated temperatures", *Eng. Fract. Mech.*, **168**, 73-91. <https://doi.org/10.1016/j.engfracmech.2016.09.006>
- Ohno, N. and Wang, J.D. (1993), "Kinematic Hardening Rules With Critical State of Dynamic Recovery. Part II: Application to Experiments of Ratcheting Behavior", *Int. J. Plast.*, **9**, 391-403. [https://doi.org/10.1016/0749-6419\(93\)90043-P](https://doi.org/10.1016/0749-6419(93)90043-P)
- Pan, L. and Seshadri, R. (2001), "Limit Load Estimation Using Plastic Flow Parameter in Repeated Elastic Finite Element Analysis", *ASME J. Pressure Vessel Technol.*, **124**, 433-439. <https://doi.org/10.1115/1.1499960>
- Peng, H.Y., Zheng, X.T., Yu, J.Y., Xu, J.M., Wang, C.G. and Lin, W. (2015), "Ratchet Limit Estimation of Pressurized Pipes under Cyclic Bending Moment", *Procedia Eng.*, **130**, 1224-1232. <https://doi.org/10.1016/j.proeng.2015.12.294>
- Ponter, A.R.S. and Chen, H. (2001), "A minimum theorem for cyclic load in excess of shakedown, with applications to the evaluation of a ratchet limit", *Eur. J. Mech. A/Solids*, **20**, 539-553. [https://doi.org/10.1016/S0997-7538\(01\)01161-5](https://doi.org/10.1016/S0997-7538(01)01161-5)
- Prager, W. (1956), "A new method of analyzing stresses and strains in work-hardening plastic solids", *J. Appl. Math.*, **23**, 493-496.
- RCC-MR (2007), Design rules for class 1 equipment, RCC-MR codes, revision.
- Reinhardt, W. (2008), "A noncyclic method for plastic shakedown analysis", *J. Press. Vess. – T. ASME*, **130**(3), 031209. <https://doi.org/10.1115/1.2937760>
- Reinhardt, W.D. and Seshadri, R. (2003), "Limit load bounds for the m_n multipliers", *J. Press. Vess. – T. ASME*, **125**, 11-18. <https://doi.org/10.1115/1.1526858>
- Seshadri, R. and Mangalaramanan, S. (1997), "Lower bound limit loads using variational concepts: the m_n method", *Int. J. Pres. Ves. Pip.*, **71**, 93-106. [https://doi.org/10.1016/S0308-0161\(96\)00071-3](https://doi.org/10.1016/S0308-0161(96)00071-3)
- Shen, J., Chen, H.F. and Liu, Y.H. (2018), "A new four-dimensional ratcheting boundary: Derivation and numerical validation", *Eur. J. Mech. - A/Solids*, **71**, 101-112. <https://doi.org/10.1016/j.euromechsol.2018.03.005>
- Varvani-Farahani, A. and Nayebi, A. (2017), "Ratcheting in pressurized pipes and equipment: A review on affecting parameters, modelling, safety codes, and challenges", *Fatigue Fract. Eng. Mater. Struct.*, **41**, 503-538. <https://doi.org/10.1111/ffe.12775>
- Wolters, J., Breitbach, G., Roding, M. and Nickel, H. (1997), "Investigation of the ratcheting phenomenon for dominating bending loads", *Nucl. Eng. Des.*, **174**, 353-363. [https://doi.org/10.1016/S0029-5493\(97\)00128-3](https://doi.org/10.1016/S0029-5493(97)00128-3)
- Yamamoto, Y., Yamashita, N. and Tanaka, M. (2002), "Evaluation

- of thermal stress ratchet in plastic FEA", *ASME PVP*, **439**, 3-10. <https://doi.org/10.1115/PVP2002-1215>
- Zakavi, S.J., Shiralivand, B. and Nourbakhsh, M. (2017), "Evaluation of combined hardening model in ratcheting behavior of pressurized piping elbows subjected to in-plane moments", *J. Compos. Appl. Res. Mech. Eng.*, **7**(1), 57-71. <https://doi.org/10.22061/JCARME.2017.640>
- Zheng, X.T., Peng H.Y., Yu J.Y., Wang, W., Lin, W. and Xu, J.M. (2017), "Analytical ratchet limit for pressurized pipeline under cyclic nonproportional loadings", *J. Pipeline Syst. Pract.*, **8**(3), 04017002. [https://doi.org/10.1061/\(ASCE\)PS.1949-1204.0000260](https://doi.org/10.1061/(ASCE)PS.1949-1204.0000260)

CC

Acronyms

C-TDF	Committee of Three Dimensional Finite Element Stress Evaluation
ASME	American Society of Mechanical Engineer
KTA	Kerntechnischer Ausschuß
RCC-MR	Design and Construction Rules for Power Generating Stations
LMM	linear matching method
UMY	Uniform Modified Yield method
LDYM	Dependent Yield Modification method
OW II model	Ohno-Wang II model

Nomenclature

D_i	Inner diameter of the straight pipe	q_i	Elastic modulus adjustment parameter
D_o	Outer diameter of the straight pipe	r_i	Inside radius of pipe
E	Elastic modulus	r_o	outside radius of pipe
E^{i+1}	Elastic modulus of i^{th} element	ΔF	Bending loading range
F_{sy}	Secondary bending stress range for the straight pipe or elbow	ΔQ	Secondary bending stress range
K	The ratio of outside radius and inside radius of pipe $K = r_o/r_i$	$\Delta\sigma_{eq}$	von Mises stress distribution of each element
L_s	The distance from the reversed bending loading point to the connecting section of straight pipe and elbow pipe	ϵ_{eq}	Equivalent strain of each element of each elastic iteration
P	Internal pressure	θ	The angle of elbow pipe
P_b	Primary bending stress	ν	Poisson's ratio
P_{eff1}	Effective primary stress	ν_1	The ratio of primary membrane stress and effective primary stress
P_m	Primary membrane stress	σ_{eq}	von Mises stress of each element of each elastic iteration
P_{sy}	Corresponds to the pressure value at which the straight pipe with the same schedule yields at inner surface	$(\sigma_{eq})_{\max}$	von Mises stress of each element of each elastic iteration
$R_L = m_2^0/m_L$	The ratio of limit load multiplier m_2^0 and lower limit load multiplier m_L	$(\sigma_{ref})^i$	Reference stress of i^{th} element
$R_0 = m_2^0/m$	The ratio of limit load multiplier m_2^0 and exact multiplier m	σ_y	Yield strength
$R_\alpha = m_\alpha/m$	The ratio of limit load multiplier m_α and exact multiplier m	σ'_y	Modify the yield strength $\sigma'_y = \sigma_y - \Delta\sigma_{eq}/2$
R_i	Internal diameter of thick wall cylinder		
R_o	outer diameter of thick wall cylinder		
S_m	Allowable stress		
SR_1	The ratio of secondary stress and membrane stress		
X	The ratio of primary membrane stress and the pressure value		
l_i	the spans of the lower and upper clips in Fig. 1		
l_o	the spans of the lower and upper clips in Fig. 1		
i	Iteration number		
m	Exact multiplier		
m_2^0	Limit load multiplier		
m_L	Lower limit load multiplier		
m_α	Limit load multiplier		